DMD Fast Forward. Published on October 29, 2009 as doi:10.1124/dmd.109.028928

Coupling of LC-MS/MS and LC-SPE-NMR techniques for the structural identification of metabolites following *in vitro* biotransformation of SUR1-selective K_{ATP} channel openers

Florian Gillotin, Patrice Chiap, Michel Frédérich, Jean-Claude Van Heugen, Pierre Francotte, Philippe Lebrun, Bernard Pirotte and Pascal de Tullio

Drug Research Center (CIRM), Laboratoire de Chimie Pharmaceutique et Laboratoire de Pharmacognosie, Université de Liège (M.F., P.F., B. P., P. de T.)

Laboratoire de Pharmacodynamie et de Thérapeutique, Université Libre de Bruxelles (P.L.).

A.T.C. s.a. (Advanced Technology Corporation), Academic Hospital of Liège (CHU) (F.G., J.C. V. H., P.C.).

Running Title:

LC-MS/MS and LC-SPE-NMR for identification of SUR1 PCOs *in vitro* metabolites.

Corresponding author: de Tullio Pascal, Drug Research Center (CIRM), Laboratoire de Chimie Pharmaceutique, Université de Liège, 1 avenue de l'hôpital, B-4000 Liège, Belgium. Tel: 32-(0)4-366-43-69. Fax: 32-(0)4-366-43-62. E-mail: P.deTullio@ulg.ac.be

Statistics

Number of text pages: 23

Number of tables: 2

Number of Figures: 6

Number of references: 28

Words in abstract: 207

Words in introduction: 1106

Words in discussion: 2892

List of non-standard abbreviations

PCOs: Potassium Channel Openers

ADMET: Absorption, distribution, Metabolism, Excretion, Toxicity

SPE : Solid-Phase Extraction

TRIS : 2-amino-2-hydroxyméthyl-1,3-propanediol

CYPs: cytochrome P450 enzymes

PB: Phenobarbital

NAD: Nicotinamide adenine dinucleotide

NADP: Nicotinamide adenine dinucleotide phosphate

ACN: Acetonitrile

DMD Fast Forward. Published on October 29, 2009 as DOI: 10.1124/dmd.109.028928
This article has not been copyedited and formatted. The final version may differ from this version.

ABSTRACT

SUR1-selective ATP-sensitive potassium channel openers (PCOs) have been shown to be of clinical value for the treatment of several metabolic disorders, including type I and type II diabetes, obesity and hyperinsulinemia. Taking into account these promising therapeutic benefits, different series of 3-alkylamino-4*H*-1,2,4-benzothiadiazine 1,1-dioxides structurally related to diazoxide were developed. In view of the lead optimisation process of the series, knowledge of ADMET parameters, and more particularly the metabolic fate of these compounds, is a fundamental requirement. For such a purpose, two selected promising compounds (BPDZ 73 and BPDZ 157) were incubated in the presence of phenobarbital-induced rat liver microsomes to produce expected mammal *in vivo* phase I metabolites. The resulting major metabolites were then analysed by both MS and NMR in order to completely elucidate their chemical structures. The two compounds were also further incubated in the presence of non-treated rats and human microsomes in order to compare the metabolic profiles. In the present study, the combined use of an exact mass LC-MS/MS platform and a LC-SPE-NMR system allowed the clarification of some unresolved structural assessments in the accurate chemical structure elucidation process of the selected PCOs drugs. These results greatly help the optimization of the lead compounds.

DMD Fast Forward. Published on October 29, 2009 as DOI: 10.1124/dmd.109.028928
This article has not been copyedited and formatted. The final version may differ from this version.

INTRODUCTION

ATP-sensitive potassium channels (K_{ATP} channels) found in a wide range of cell types are regulated by changes in intracellular adenosine triphosphate (ATP) concentrations (Miki et al., 1999; Ballanyi, 2004; Ardehali and O'Rourke, 2005; Billman, 2008; Ko et al., 2008). These channels are formed by the combination of two different subunits, Kir6.x and SURx, the latter containing the regulatory sites for most channel modulators (Babenko et al., 1998). Several isoforms of Kir6.x (Kir6.1 and Kir6.2) and SURx (SUR1, SUR2A, SUR2B) have been reported (Inagaki et al., 1995; Hambrock et al., 1999). The Combination of these different subunits led to specific K_{ATP} channel subtypes. Activation of K_{ATP} channels creates an increase in the outflow of potassium ions through the cytoplasmic membrane and, consequently, an increase in membrane polarisation. The physiological impact of this hyperpolarisation is dependent on the tissue localization of the channel but generally results in a reduction of cell excitability. As a result, potassium channel openers (PCOs) can interfere with several important physiological processes such as insulin release from pancreatic B-cells and contractile activity from smooth muscle cells (Lawson, 1996; Lebrun et al., 1997). Selective activation of pancreatic K_{ATP} channels has been shown to be of therapeutic value for the treatment of metabolic disorders such as diabetes, obesity and hyperinsulinaemia (Rasmussen et al., 2000; Hansen, 2006). Taking into account these potential therapeutic benefits, a series of new compounds belonging to the 3-alkylamino-4*H*-1,2,4-pyrido- and 3-alkylamino-4*H*-1,2,4-benzothiadiazine 1,1-dioxides were developed during the last decade by our group. Among these drugs, BPDZ 44 (**1**), BPDZ 73 (**2**), BPDZ 154 (**3**), BPDZ 157 (**4**), BPDZ 415 (**5)** and BPDZ 256 (**6)** (Figure 1) were identified as potent and selective pancreatic PCOs (Pirotte et al., 1994; de Tullio et al., 2003; de Tullio et al., 2005). However, in spite of their excellent *in vitro* profiles, many of these compounds exhibited unexpected *in vivo* results in terms of potency and/or side effects. These negative results could be explained by unfavorable pharmacokinetic or metabolic properties. Therefore, within the drug discovery and the lead

DMD Fast Forward. Published on October 29, 2009 as DOI: 10.1124/dmd.109.028928
This article has not been copyedited and formatted. The final version may differ from this version.

optimisation process of these interesting drugs, the study of their metabolism and more especially the determination of the metabolites chemical structures appears to be essential. Indeed, the knowledge of the metabolic brittleness zones could be relevant in order to suppress or to reduce the formation of undesirable metabolites. Early knowledge of *in vitro* metabolism during the drug design process is also helpful to assist transition from *in vitro* to *in vivo* studies.

For these purposes, the BPDZ 73 and BPDZ 157 *in vitro* metabolic profiles were studied using liver microsomes. In a first step, parent compounds were incubated in the presence of Phenobarbital-induced rat liver endoplasmic reticulum vesicles (microsomes) since this is a very well established method to produce expected *in vivo* phase I metabolites. Indeed, phenobarbital treatment increases the expression level of the majority of drug metabolising enzyme cytochromes P450 (CYPs) (Waxman and Azaroff, 1992). Therefore, the use of such liver microsomes is expected to produce *in vivo* phase I metabolites in large amounts. As *in vivo* screenings are conducted in rats, metabolism was studied, in a second step, using non-induced rat liver microsomes in order to highlight the putative relationships between the *in vivo* activity and the drugs metabolic fate. Finally, to extrapolate results to the human species, incubation of the parent compounds was also conducted in the presence of pooled human liver microsomes.

Usually, the major metabolites generated during incubation are analysed by liquid chromatography (LC) coupled to a mass spectrometer (Oliveira, 2000; Clarke et al., 2001). Nevertheless, some specific structural modifications remain very difficult to determine using this approach. So, other analytical techniques are required to resolve the complete chemical structures of metabolites. It is well known that for organic compounds, ^{1}H and/or ^{13}C NMR spectroscopy is the most powerful, the most helpful and the simplest method for structural analysis. Despite its great interest, the relative poor sensitivity of NMR and the technical difficulty to directly combine this instrument to a LC system has not permitted the use of this technical approach for a long time, especially with small amounts of compounds. The classical method used to obtain NMR data for major compounds from a mixture was to use a preparative-scale

DMD Fast Forward. Published on October 29, 2009 as DOI: 10.1124/dmd.109.028928
This article has not been copyedited and formatted. The final version may differ from this version.

(or semi-preparative-scale) separation and purification, to evaporate the mobile phase and to dissolve the residues in a deuterated solvent before classical NMR tube analysis. Even if this method appears to be quite simple and has been applied with relative successes for a long time, several disadvantages could be noticed: the work-up step could be very time consuming, the evaporation step could generate some negative chemical reactions (i.e. oxidation, solvolysis, degradation…) that could deteriorate the nature of the analyte and could concentrate into the solution non-desired compounds (i.e. salts and/or solvent impurities). Recently, the developments of the hyphenated LC-NMR and particularly of LC-SPE-NMR have enhanced its possible applications to mixtures separation and resolution (Corcoran and Spraul, 2003; Silva Elipe, 2003; Simpson et al., 2004). The introduction of a solid phase extraction step between LC and NMR was shown to be attractive and efficient especially in terms of time consumption and sensitivity (Clarkson et al., 2005; Sandvoss et al., 2005). The main advantages of LC-SPE-NMR in comparison to classic LC-NMR and conventional preparative step-tube NMR are as follows: possible complete automation and hyphenation, increased sensitivity (i.e. due to multi-trapping process and to a concentration effect linked to a highly concentrated re-elution band), elimination of the LC solvents by flushing the cartridges with water to remove acids from the elution buffer, avoidance of contaminations and flush with deuterated solvent (reduction of salt and/or impurities negative effects and use of classical NMR sequences), minimization of artefacts due to possible degradations. In addition, LC separations can be carried out under optimized and typical liquid chromatography conditions and the non-deuterated solvents can be evaporated completely. This procedure reduces the need for residual solvent suppression and guarantees an optimal quality of the recorded NMR spectra. However, the SPE step (trapping and re-elution) has to be developed very carefully and could be sometimes the limitative and the time consuming step of the process, especially with unknown products or very polar compounds (Wilson et al., 2006). In spite of these disadvantages, LC-SPE-NMR, coupled with LC-MS/MS techniques remains a convenient platform for accurate chemical structure elucidation (Barbuch et al., 2006; Yang, 2006; Tatsis et al., 2007). We decided to use such a platform for metabolism studies of

DMD Fast Forward. Published on October 29, 2009 as DOI: 10.1124/dmd.109.028928
This article has not been copyedited and formatted. The final version may differ from this version.

SUR1-selective benzothiadiazine 1,1-dioxides. Among those, BPDZ 73 and BPDZ 157 were chosen, according to structural features and pharmacological interest, for an *in vitro* evaluation of their metabolism. Their major metabolites were then analysed using both LC-MS/MS (quadrupole - time of flight mass spectrometer (Q-TOF)) and LC-SPE-NMR.

METHODS

Chemicals and reagents

The compounds BPDZ 73 (7-chloro-3-isopropylamino-4*H*-1,2,4-benzothiadiazine 1,1-dioxide) and BPDZ 157 [7-chloro-3-(3-pentylamino)-4*H*-1,2,4-benzothiadiazine 1,1-dioxide] have been synthesized at the Drug Research Center (Laboratoire de Chimie Pharmaceutique) of the Université de Liège. Acetonitrile and methanol of HPLC grade were obtained from Biosolve B.V. (Valkenswaard, The Netherlands). NAD, NADP and glucose-6-phosphate dehydrogenase were bought from Roche Diagnostics Gmbh (Mannheim, Germany). Glucose-6-phosphate, ammonium formate, EDTA, TRIS, sucrose and leucine-enkephalin were obtained from Sigma (St. Louis, MO, USA). Formic acid and phosphoric acid were of an analytical grade from Merck (Darmstadt, Germany). Phenobarbital (PB) was provided by Certa (Braine-l'Alleud, Belgium). Deuterated acetonitrile was purchased from Euriso-Top (Gif sur Yvette, France). Phenobarbital induced rat liver microsomes were isolated from male Sprague-Dawley rats (± 300 g) treated with PB (50 $mg.kg^{-1}$) administered i.p. daily, for 4 days. Twenty-four hours after the final treatment, rats were killed and their livers excised, blotted dry, weighed, then minced and homogenized in 4 volumes of ice-cold homogenization buffer (TRIS 0.01M; sucrose 0.25M, EDTA 0.1mM; pH 7.4) using a Potter apparatus. The homogenate was centrifuged (9000 g) for 20 min at 4°C. The supernatant was isolated and further centrifuged (106,000 g) for 60 minutes at 4°C. The pellet was suspended in an ice-cold homogenization buffer and the suspension was re-centrifuged (106,000 g) for 40 minutes at 4°C. Microsomal pellets were finally re-suspended in 0.1 M TRIS buffer

(pH 7.4) containing 0.1 mM EDTA to yield a protein concentration of approximately 16 to 24 mg/ml. Non-induced rat liver microsomes came from our library and were produced following the same steps. Pooled Human liver microsomes were supplied by BD Biosciences Europe (Erembodegem, Belgium).

Metabolism

The preferred *in vitro* biological test system selected to metabolise the parent compounds (BPDZ 73 and BPDZ 157) was the phenobarbital (PB) induced male rat liver microsomes system. The parent compounds were dissolved in methanol and added directly to the incubation medium in order to reach a final substrate concentration of 200 µM and a final percentage in methanol lower than 1 %. The incubations were performed at 37°C in a water shacking bath with a final protein content of 1mg/ml in a total volume of 1 ml. The reactions were initiated by addition of a NADPH regenerating system. The reactions were stopped after an incubation time of 60 minutes by addition of 1 ml of methanol and 2 ml of acetonitrile and by a subsequent vortexing step. Samples were further centrifuged at 2000 g for 5 minutes. The supernatant was further decanted into a glass tube and organic solvents were evaporated under an inert nitrogen flux in order to concentrate the samples. The residue was finally redissolved in 300 µl of a mixture composed of 10 mM ammonium formate buffer (pH 3.0) and acetonitrile (50/50; v/v). Non-incubated samples (T_0) were also prepared for comparison. These samples were prepared by the addition of methanol and acetonitrile before supplementing the incubation medium with the NADPH regenerating system. The same experimental procedure was applied to parent compounds in the presence of non-induced rat and pooled Human liver microsomes.

LC-MS/MS conditions

DMD Fast Forward. Published on October 29, 2009 as DOI: 10.1124/dmd.109.028928
This article has not been copyedited and formatted. The final version may differ from this version.

The LC analyses were carried out on an HPLC Alliance 2695 system obtained from Waters (Milford, MA, USA). The samples (10 µl) were injected by an autosampler and the analytes were separated using a Luna C18 analytical column (150 x 4.6 mm, i.d.; particle size = 5 µm) from Phenomenex (Torrance, CA, USA) with a mixture of two mobile phases: (A) 0.2 % formic acid / methanol (95/5; v/v) and (B) acetonitrile. The following linear elution gradient was applied: 0 min, 0 % ACN; 30 min, 95 % ACN; 35 min, 95 % ACN; 35.10 min, 100 % ACN; 45.10 min, 100 % ACN. The column was then re-equilibrated with 100 % of the mobile phase A for a 10 minutes period with initial conditions prior to the next injection. The flow-rate was 0.5 ml/min. The column temperature was set to 40°C. A Q-Tof II mass spectrometer from Micromass (Manchester, UK) operating in positive electrospray ionisation mode was directly coupled to the LC device. The metabolite detection was performed by monitoring the total ionic current (TIC) within 0.5 seconds regular intervals and a range *m/z* extending from 90 to 650. The optimum cone voltage was 31 V. Collision induced dissociation (CID) was performed using a collision energy ramp between 20 and 25 eV with Ar as the collision gas. For accurate mass measurements, the mass spectrometer was calibrated with a mixture of 0.1 % phosphoric acid and ACN (50/50; v/v) to give a resolution of about 9000. Leucine-enkephalin (*m/z* 556.227) was used for lock-mass correction during accurate mass measurements of detected metabolites as well as their product ions resulting from CID. All the data acquisitions were achieved using MassLynx Version 4.1 software from Waters.

LC-SPE-NMR conditions

The LC-SPE-NMR platform used is a completely hyphenated and on-line system. The LC separations were carried out on an Agilent 1100 series liquid chromatography system from Agilent (Waldbronn, Germany) equipped with a quaternary pump, a column thermostat, an autosampler and a diode array detector. The analyte separations were performed on an Alltech Hypersil BDS C18 column (150 x 4.6 mm, i.d.; particle size = 3 µm) from Alltech (Breda, The Netherlands) using mobile phase A:

DMD Fast Forward. Published on October 29, 2009 as DOI: 10.1124/dmd.109.028928
This article has not been copyedited and formatted. The final version may differ from this version.

10 mM ammonium formate pH 3.0 and mobile phase B: acetonitrile (ACN) with a flow-rate of 0.8 ml/min and the following linear gradient: 0 min, 10% ACN; 24 min, 40% ACN; 27 min, 60% ACN and 30 minutes, 10% ACN. The column temperature was set to 40°C. The eluate followed the flow path to a Prospekt II automated solid phase extraction (SPE) unit from Bruker/Spark Holland (Emmen, The Netherlands) under the control of Bruker Hystar 3.0 software. To ensure that the used SPE conditions were adapted to the tested compounds, it was initially verified that the (multi)trapping and the elution steps with small and defined quantities of the parent compounds (10 to 30 µg injected) led to ^{1}H NMR spectra with sufficient signal-to-noise ratio to obtain reliable integration of each signal within a reasonable scan accumulation. Indeed, the nature of the SPE cartridge had to be chosen, the flow rate of water added during trapping to the mobile phase had to be adjusted and the nature of the eluting deuterated solvent had to be defined. Taking into account this data, the minimal amount of metabolites was estimated to obtain useful 1D and 2D NMR spectra and the experimental conditions were defined. From this work, it appears that a minimal quantity of 20 µg injected is required for each metabolite. Then a concentrated solution has been prepared by pooling together 20 incubated samples before evaporation under an inert nitrogen flux. The residue was redissolved in 500 µl of a mixture composed of 10 mM ammonium formate pH 3.0 and acetonitrile (50/50; v/v), vortexed, centrifugated at 2000 g for 5 minutes. The supernatant was decanted and used as an injection solution. The peaks of interest (detected using the U.V. response at 254 nm) were trapped on Hysphere GP cartridges (10 mm × 2 mm) from Spark Holland (Emmen, The Netherlands) by addition of water at a 2 ml/min flow-rate to the post-column eluate. Three consecutive injections (80 µl per injection) were trapped on the same cartridge in order to enhance the metabolite concentration. After the trapping process, the cartridges were dried under a constant nitrogen flow to remove residual non-deuterated solvents. The collected fractions were further directly transferred from the SPE cartridges to the NMR cell probe with 290 µl of ACN-d_3. The NMR measurements were carried out using an AV500 MHz spectrometer from Bruker BioSpin (Rheinstetten, Germany) equipped with a 3 mm (60 µl) dual inverse ^{1}H/^{13}C z-gradient flow probe.

^{1}H NMR experiments

^{1}H NMR sequence was used with a pulse width of 30 °, a relaxation delay of 2 s and 64 K data points processed into 32 K points with exponential line broadening of 0.3 Hz. A double presaturation NOESY pulse sequence (lc1pncwps) adapted to SPE with shaped pulses for suppression of acetonitrile and water signals was also used to obtain spectra with enhanced signal-to-noise ratio. ^{13}C decoupling was applied to eliminate ^{13}C satellites of the solvents. The spectral window was 10 KHz with 16 K data points processed into 32 K points using zero filling and exponential line broadening of 1 Hz. The number of scans was adapted to obtain the appropriate signal to noise ratio.

Two dimensional COSY spectra were acquired without solvent presaturation using the magnitude mode sequence. The spectra were recorded with a spectral window of 7 KHz in both dimensions and transferred into 1K data points with 128 increments. Data were zero-filled in f1 to 1024 points and processed using the sine bell function with exponential line broadening of 0.3 Hz in f1 and 1 Hz in f2.

RESULTS

Compounds BPDZ 73 and BPDZ 157 were submitted to biotransformation and subsequent analysis but, to avoid repetition and dispersion, the LC-MS/MS and LC-SPE-NMR results will be mainly focused on BPDZ 157 incubated in the presence of Phenobarbital-induced rat liver microsomes which could be considered as the most interesting biotransformation profile in terms of metabolism complexity. Only the final results concerning the metabolic profiling of BPDZ 73 will be presented and further discussed.

***in vitro* metabolism**

DMD Fast Forward. Published on October 29, 2009 as DOI: 10.1124/dmd.109.028928
This article has not been copyedited and formatted. The final version may differ from this version.

Biotransformation of BPDZ 157 was performed by incubation of the compound in the presence of Phenobarbital-induced male rat liver microsomes and a NADPH generating system. Following the incubation step, the samples were analysed by LC. Metabolite products highlighting was made possible by comparing chromatograms of samples having undergone or not (T_0 samples) a biotransformation mediated by rat liver microsomes. T_0 samples were prepared like the other samples but CYPs were inactivated by addition of acetonitrile and methanol before starting the biotransformation reactions. As a result, no biotransformation occurred in these samples.

As shown in Figure 2, the parent product BPDZ 157 is eluted at a retention time of about 25 minutes (relative retention time = 1). The comparison between the chromatograms of samples that have undergone or not CYP-mediated biotransformation for an incubation period of 1 hour highlights, the presence of 6 major metabolites absorbing at 254 nm (cf. Figure 2). These products were named M1 to M6, according to their elution order, and were characterized by relative retention times (RRT) and estimated percentages of 0.47 (3 %); 0.58 (2 %); 0.69 (10 %); 0.70 (18 %); 0.73 (15 %) and 0.79 (2 %), respectively. As expected in reversed-phase LC, the RRT of these peaks were lower than that of the parent product, which indicates that the metabolites are more polar compounds.

Metabolism of BPDZ 157 was also studied using microsomes from non-induced rat and pooled Human liver. Metabolites M1 to M6 were also detected in the metabolisation profile recorded for samples resulting from BPDZ 157 incubation in the presence of non-treated rat liver microsomes (data not shown). Nevertheless, all metabolites were produced in smaller amounts, which reinforces the utility of using Phenobarbital-induced liver microsomes in the metabolite chemical structure elucidation process. Incubation of BPDZ 157 in the presence of pooled Human liver microsomes results in the production of the major metabolites M3 to M6. Metabolites M1 and M2 were not detected with the used techniques but, interestingly, two new minor metabolites (named M7 and M8) were highlighted in human species (data not shown). Since the latter were produced in small amount, no further inquiries were conducted here to elucidate their chemical structures.

DMD Fast Forward. Published on October 29, 2009 as DOI: 10.1124/dmd.109.028928
This article has not been copyedited and formatted. The final version may differ from this version.

LC-MS/MS analyses of BPDZ 157

The mass spectrometer was initially used in TOF scan mode to determine the molecular masses of peaks eluted during chromatographic separations by TIC monitoring. The BPDZ 157 metabolites M3, M4 and M5 were all characterized by a protonated molecule $[M+H]^+$ at *m/z* = 318 higher than for the parent compound ($[BPDZ\ 157 + H]^+$ at *m/z* = 302) and were equivalent to the mass increment of an oxygen atom. Since the CYP-mediated reaction involves the combination of oxygen with the organic substrate to produce a molecule of water and a mono-oxygenated metabolite, the mass increment of these biotransformation products can be explained by the introduction of one oxygen atom on the chemical structure of the parent compound BPDZ 157 to form a hydroxyl group. The protonated molecule $[M+H]^+$ of M2 exhibited a *m/z* of 334, which corresponds to a mass increment equivalent to two oxygen atoms (32 Da) and introduction of two hydroxyl groups on the parent chemical structure. The metabolite M1 had a mass of 232 Da, which is equivalent to the loss of 70 Da by BPDZ 157 and which could result from the removal of the pentyl side chain. Finally, the M6 metabolite was characterized by a $[M+H]^+$ at *m/z* = 316.

In order to validate those assumptions and to localize structural modifications induced by the CYPs, the product ion spectra in TOF MS/MS mode of each metabolite and the parent compound were further performed (Table 1 summarize the MS/MS results obtained with the parent BPDZ 157 and its major metabolites). As illustrated in Figure 3 (A), the product ion spectrum of $[BPDZ\ 157+H]^+$ (*m/z* = 302) showed a series of signals at m/z = 126, 142, 190 and 232. The product ions at *m/z* = 232, 190, 142 and 126 were issued from the loss of 70 Da (C_5H_{10}), 112 Da ($C_6H_{11}N_2$), 160 Da ($C_5H_7N_2O_2S$) and 176 Da ($C_6H_{10}N_2O_2S$), respectively. This fragmentation pathway may be explained according to Figure 3 (B). The fragmentation of the protonated molecule $[M+H]^+$ (m/z = 232) corresponding to metabolite M1 generates a series of peaks at *m/z* = 126, 142 and 190. These product ions are common to those of the parent compound and thus result from the same fragmentation mechanism. Consequently, it is probable that compound BPDZ 157 is metabolized in a compound of mass 232 Da (metabolite M1) characterized

DMD Fast Forward. Published on October 29, 2009 as DOI: 10.1124/dmd.109.028928
This article has not been copyedited and formatted. The final version may differ from this version.

by the loss of the pentyl group. The product ion spectrum of metabolite M2 (*m/z* = 334) was characterized by peaks at *m/z* = 126, 142, 190, 232, 272, 298 and 316. Since some common signals (at *m/z* = 126, 142, 190 and 232) were found in the product ion spectra of BPDZ 157 and M1, it can be concluded that the introduction of the two oxygen atoms was carried out neither on the benzene core nor on the 1,2,4-thiadiazine 1,1-dioxyde cycle but rather on the pentyl group. However, the mass spectrometry analyses do not allow to precisely localise the position of the two oxygen atoms on the alkyl side chain. The metabolites M3, M4 and M5 (*m/z* = 318) displayed similar product ion spectra which were characterized by peaks at *m/z* = 126, 142, 190, 232 and 300. As for the metabolites previously analyzed, some product ions (at *m/z* = 126, 142, 190 and 232) were common to the entities generated during MS/MS analysis of the parent compound and thus resulted from identical fragmentation pathways. Analysis of the product ion spectra of M3, M4 and M5 led to the same conclusion as that established for metabolite M2. Indeed, the existence of an identical fragmentation pathway to that of BPDZ 157 implies that the metabolites resulted from hydroxylation on carbon atoms located on the side alkyl group of BPDZ 157.

Finally, the product ion spectrum of the sixth metabolite detected (M6, *m/z* = 316) is also characterized by identical product ions to those of BPDZ 157 (peaks at *m/z* = 126 and 190) and leads to the same conclusion as that established above: a fragmentation pathway identical to that of the parent compound. By comparison with the metabolites M2, M3, M4 and M5, the mass increment detected (14 Da) for M6 can be explained by the formation of a carbonyl group. Nevertheless, the data obtained by fragmentation were not sufficient to determine the exact position of that modification. However, the presence of product ions at *m/z* = 126 and 190 allowed to conclude that such a modification is neither on the benzene core nor on the 1,2,4-thiadiazine 1,1-dioxide cycle. Figure 3C highlights the putative structures of the major BPDZ 157 metabolites.

LC-SPE-NMR analyses of BPDZ 157

As previously described, LC-MS/MS analysis of BPDZ 157 metabolites led to some uncertainties about the exact localisation of the hydroxyl groups on the alkylamino side chain. Consequently, in this case, the use of the NMR approach could be very helpful to raise the structural uncertainties.

As the NMR spectrometry technique requires larger sample quantities than mass spectrometry (more than 10 µg of each metabolite), a concentrated solution (prepared as previously described from the pool of 20 incubated samples) was used for LC-SPE-NMR analysis. The work up used to prepare the concentrated solution changed the proportions of each metabolite but did not alter the chromatographic profile.

Following chromatographic separations, each metabolite and the parent peak were collected onto SPE cartridges as a result of three consecutive injections (80 µl per injection) in a multiple trapping sequence. After drying for residual non-deuterated solvents removal, each BPDZ 157 metabolite was transferred into the NMR-probe with deuterated ACN. From the UV data obtained after LC separation of the concentrated solution and by comparison with data measured from control solution of BPDZ 157, the amount of each metabolite trapped after 3 injections was estimated as followed: M1 (~ 20 µg), M2 to M5 (~ 18-25 µg), M6 and BPDZ 157 (~ 15 µg).

Two 1D protons spectra (one using classical quantitative proton sequence and a second one using a double NOESY presaturation) and a 2D COSY spectrum were measured for each metabolite. The classical proton spectra (NS from 128 to 1024 scans, 10 min. to 1 h.) allowed the integration of each signal (if the signal-to-noise ratio was sufficient) while the double presaturation sequence furnished more sensitivity and resolution but could not be used for integration. The COSY spectra (NS from 8 to 64 scans, 25 min. to 3 h.) were important to define the proton-proton correlations.

DMD Fast Forward. Published on October 29, 2009 as DOI: 10.1124/dmd.109.028928
This article has not been copyedited and formatted. The final version may differ from this version.

Table 2 presents the chemical shifts and the proton-proton correlations obtained from the proton and COSY data and Figure 4 shows the classical proton spectra (30 ° pulse) for the different BPDZ 157 metabolites.

First of all, the similarity between the ^{1}H proton spectra of the trapped parent peak and BPDZ 157 reference in deuterated ACN was verified. The ^{1}H-NMR spectrum of BPDZ 157 is characterized by chemical shifts (δ_H) of 0.95 (protons of the two terminal methyl groups 5' and 6'), 3.79 (proton in position 2'), 5.65 (proton in position 1') and 8.87 ppm (proton in position 4). The chemical shifts of the protons located on the benzene ring are monitored between 7 and 8 ppm (7.14, 7.53 and 7.75). It is interesting to note that the proton couples located in position 3' and 4', expected to be chemically identical, appear to resonate at different δ_H values (1.64 and 1.52 ppm). This feature is corroborated by the COSY spectrum that suggests the splitting of the CH_2 group in position 3' and 4' into 2 distinct signals. It was not possible to precisely assign correspondence signals from the obtained NMR data but this observation seems to indicate that these two pairs of protons have different magnetic environments (diastereotopic protons), probably resulting from conformational isomerism.

In concern to M1, the LC-MS/MS analysis indicated a probable loss of the alkyl side chain. This putative structure was confirmed by the NMR data since no signals corresponding to the alkyl side chain were monitored in the ^{1}H spectrum and the 1' integration signal indicated the presence of two protons at this position.

The LC-MS/MS data of M2 suggested that this metabolite resulted from the introduction of 2 oxygen atoms on the BPDZ 157 chemical structure corresponding to a double hydroxylation of the alkyl side chain but could not exactly locate modifications. Examination of the proton data (Table 2) shows that, in comparison to the parent compound, the aromatic peaks are not affected. Such a feature confirms the assumption made by mass spectrometry analysis that the introduction of the two oxygen atoms was carried out neither on the benzene core nor on the 1,2,4-thiadiazine 1,1-dioxide cycle but rather on the pentyl group. NMR analysis clearly demonstrated that the two OH groups are linked to

DMD Fast Forward. Published on October 29, 2009 as DOI: 10.1124/dmd.109.028928
This article has not been copyedited and formatted. The final version may differ from this version.

position 3' and 4' of the pentyl group. This assumption is supported by the disappearance of the CH_2 signals around 1.5 ppm and the appearance of signals with up-field chemical shifts (due to the –I effect of the hydroxyl groups) and which couple with the two CH_3 located around 1.2 ppm (demonstrated by COSY analysis). Moreover, a signal that integrates for 2 protons was detected at 3.4 ppm and could be attributed to the newly introduced OH groups.

Following mass spectrometry analysis, metabolites M3, M4 and M5 were expected to be mono-hydroxylated derivatives but the position of the OH group could not be determined using the generated MS/MS data. Again, examination of the NMR spectra gave access to the exact localisation of the modification site.

The NMR spectral information generated for M3 allowed to precise that the hydroxyl group was attached on one of the terminal CH_3: disappearance of one of the CH_3 signal around 1 ppm, presence of a CH_2 signal at low shield which couples with a CH_2 signal at 1.74 ppm and presence of a putative OH signal at 2.9 ppm. In comparison to the parent compound, the aromatic peaks are not affected.

The ^1H spectral data of metabolites M4 and M5 are similar and indicate the presence of a hydroxyl group on the position 3' or 4'. Indeed, the aromatic signals of these two compounds remained unchanged and confirmed the absence of modifications on the aromatic cores although evidences for the modification of the CH_2 groups 3' or 4' could be clearly noted: disappearance of one CH_2 signal around 1.5 ppm, unfolding of the CH_3 and of one CH_2 signal, appearance of a deshielded CH (coupling with a CH_3 signal) and of a OH signal. Interestingly, BPDZ 157 structure analysis shows that introduction of a hydroxyl on the methylene group induces two stereogenic centres (in 2' and the carbon hosting the hydroxyl group). Such a feature implies the possible existence of 4 stereoisomers divided into 2 couples of enantiomers, which are diastereoisomers between them (Cf. Figure 5A).

Moreover, the NMR spectra obtained with M6 are not usable, suggesting the probable presence of more than one compound in the LC peak.

DMD Fast Forward. Published on October 29, 2009 as DOI: 10.1124/dmd.109.028928
This article has not been copyedited and formatted. The final version may differ from this version.

Metabolism of BPDZ 73

As for BPDZ 157, BPDZ 73 biotransformation step was followed by samples analysis using both LC-MS/MS and LC-SPE-NMR in order to elucidate the chemical structure of BPDZ 73 metabolites. The retention time of the parent compound was about 19.1 minutes after analysis of the T_0 and the incubated samples. Two other chromatographic peaks of strong intensity (peaks N1 and N2 corresponding to retention times of about 11.7 and 14.3 minutes with relative percentages of 48 % and 4 %, respectively) not present in the T_0 sample were also observed (Figure 6). The retention times of these peaks, lower than that of the parent compound, indicate that these metabolites are more polar.

The parent compound BPDZ 73 was further characterised by the protonated ion $[M+H]^+$ at *m/z* = 274 for which the fragmentation led to five main ion products at *m/z* = 126, 142, 190, 208 and 232. The product ion at *m/z* = 232 is clearly linked to the parent compound with a loss of 42 Da (C_3H_7) corresponding to the departure of an isopropyl group. The ion products at *m/z* = 126, 142, 190 and 208 resulted from the loss, by the native compound, of 148 Da ($C_4H_6N_2O_2S$), 132 Da ($C_3H_4N_2O_2S$), 84 Da ($C_4H_7N_2$) and 66 Da (C_4H_3N), respectively. The fragmentation of the protonated molecule $[M+H]^+$ of the metabolite N1 ($[M+H]^+$ = 232 Da) generated a series of peaks at *m/z* = 126, 142 and 190. These product ions are common to those obtained from the parent compound and thus result from the same mechanism of fragmentation. It is consequently probable that compound BPDZ 73 is metabolized into a compound of mass 232 Da (N1 metabolite) due to the loss of an isopropyl group. The metabolite N2 is characterised by a protonated molecule $[M+H]^+$ at *m/z* = 290. The fragmentation of metabolite N2 generated peaks at m/z = 126, 142, 190, 209, 232 and 273. Three of those are common with the product ions of the parent compound, which indicates that the 16 Da mass increment detected for N2 is localised on the alkyl side chain. As for BPDZ 157, a comparison of NMR spectra of each metabolite and the parent compound allowed to identify the structural changes undergone by BPDZ 73 during the biotransformation step.

DMD Fast Forward. Published on October 29, 2009 as DOI: 10.1124/dmd.109.028928
This article has not been copyedited and formatted. The final version may differ from this version.

Analysis of ^{1}H NMR spectrum of the N1 metabolite confirms the results obtained by mass spectrometry, namely that this compound is obtained by the loss of an isopropyl group (Figure 6). The N2 metabolite was generated in lower quantity than N1 and only a small amount close to the detection limit had been harvested by the LC-SPE-NMR method. However, longer acquisition times allowed to circumvent this technical problem and to obtain results enabling chemical structure elucidation of this metabolite. Since the quantity of metabolite N2 was relatively low, no COSY spectrum could be obtained to precisely allocate the hydroxyl group introduction on the BPDZ 73 chemical structure.

Incubation of BPDZ 73 in the presence of non-treated rat liver microsomes exhibited a similar profile to that obtained with Phenobarbital-induced liver microsomes although all metabolites were produced in smaller amounts. The N1 and N2 metabolites were also highlighted in the samples resulting from incubation of BPDZ 73 with pooled human liver microsomes but, interestingly, two other minor metabolites were also detected in these samples. Nevertheless they were produced in too small amounts and further chemical structure elucidation was not considered.

DISCUSSION

The complete elucidation of the chemical structure of metabolites obtained with two benzothiadiazine dioxide-type PCOs (BPDZ 73 and BPDZ 157) after incubation with rat liver microsomes (expected phase I metabolites) was achieved by use of two complementary techniques: LC-MS/MS and LC-SPE-NMR.

LC-MS/MS provided information on the molecular mass of each metabolite and on chemical structure by examining their respective fragmentation pathway. However, in several cases, such information was not sufficient to achieve a complete elucidation of their chemical structure. Concretely, in the present study, the MS analysis indicated that compound BPDZ 157 generated six major metabolites from which three of them exhibited the same molecular mass and the same fragmentation

DMD Fast Forward. Published on October 29, 2009 as DOI: 10.1124/dmd.109.028928
This article has not been copyedited and formatted. The final version may differ from this version.

pathway. These metabolites were expected to result from the addition of one oxygen atom on a carbon atom of the alkylamino side chain at the 3-position leading to hydroxylation in an undefined position. It was demonstrated that the chromatographic separation of these metabolites and their trapping on individual SPE cartridges following by elution of the trapped metabolites with an appropriate deuterated solvent before NMR recording provided complementary information for a complete elucidation of the structure of the three hydroxylated metabolites of BPDZ 157. The biotransformation profile of compound BPDZ 157 is shown in Figure 5B. This data demonstrates that an important percentage of the parent compound is rapidly transformed. While no oxidation occurred on the benzenic ring, the alkylamino side chain at the 3-position appears to be the main metabolic brittleness of 3-alkylamino-4*H*-benzothiadiazine 1,1-dioxides. M1, M2 and M3 structures are completely resolved while we can conclude that biotransformation products M4 and M5 are probably diastereoisomers. Unfortunately, the stereochemistry of each of these metabolites could not be solved using the collected data..

This study also highlights the importance of NMR and MS data for the complete structural determination of the metabolites.

The study of the metabolism of BPDZ 73 has demonstrated the rapid biotransformation of this lead compound into one major metabolite corresponding to 3-amino-7-chloro-4*H*-benzothiadiazine 1,1-dioxide (N1). Some 3-amino-substituted benzothiadiazine 1,1-dioxides have been described in the literature to have potent hypotensive effect in a rat *in vivo* model (Raffa L, 1965). These data could be in accordance with the unexpected hypotensive effect of SUR1-selective 3-alkylamino-benzothiadiazine 1,1-dioxides. In contrast, the minor metabolite (N2) of BPDZ 73 was shown to be structurally identical to BPDZ164, a potent and selective pancreatic PCO *in vitro*. Indeed, comparing the ^{1}H NMR spectrum of N2 to that of a synthetic compound of similar structure (BPDZ164) confirmed the structural hypothesis. Consequently, N2 is clearly a compound hydroxylated on one of the two methyl groups of the alkyl chain at the 3-position (Figure 6). Introduction of such a group induces the apparition of one

stereogenic centre. Nevertheless, the stereochemical structure of N2 could not be determined by using the measured MS and NMR data.

This work also showed that the use of Phenobarbital-induced liver microsomes allows the production of large amounts of biotransformation products, easily highlighted minor metabolites and facilitated the chemical structure elucidation process. Observation of similar major metabolites in rat and human species reinforces and confirms the choice of rat species for further *in vivo* investigations.

We can conclude that the combined use of rat PB-induced microsomes model with LC-MS/MS and LC-SPE-NMR analysis, constitutes a convenient and rapid approach for identifying and elucidating the chemical structure of SUR1-selective PCO metabolites generated in classical *in vitro* conditions. This study has especially demonstrated the rapid biotransformation of 3-alkylamino-4*H*-1,2,4-benzothiadiazine 1,1-dioxides through hydroxylation and/or dealkylation of the alkylamino side chain.

Taking into account these data and informations from the literature, it appears that an enhancement of the metabolic stability of the side chain at the 3-position could be required to avoid or reduce undesired *in vivo* side effects. For that purpose, some chemical modifications of the alkylamino chain have been conducted. Compounds bearing a 1-methylcyclopropylamino or a 2-fluoroethylamino group at the 3-position have been synthesized and evaluated in terms of metabolic stability and activity. The presence of such substituents drastically reduced the total amount of generated phase 1 metabolites (using the Phenobarbital induced rat microsomes model) and especially the non-wished *N*-dealkylated derivatives (data not shown). Moreover, the introduction of a 2-fluoroethylamino side chain maintained a very interesting pharmacological profile (data not shown). By pointing the metabolic brittleness zones of 3-alkylamino-4*H*-benzothiadiazine 1,1-dioxides, this work has greatly helped the lead optimization process of the SUR1-selective PCOs, giving access to new improved drug candidates.

ACKNOWLEDGMENTS

The technical assistance of Y. Abrassart, S. Counerotte and D. Lacroix is gratefully acknowledged.

References.

Ardehali H and O'Rourke B (2005) Mitochondrial K(ATP) channels in cell survival and death. *J Mol Cell Cardiol* 39:7-16.

Babenko AP, Aguilar-Bryan L and Bryan J (1998) A view of sur/KIR6.X, KATP channels. *Annu Rev Physiol* 60:667-687.

Ballanyi K (2004) Protective role of neuronal KATP channels in brain hypoxia. *J Exp Biol* 207:3201-3212.

Barbuch RJ, Campanale K, Hadden CE, Zmijewski M, Yi P, O'Bannon DD, Burkey JL and Kulanthaivel P (2006) In vivo metabolism of [14C]ruboxistaurin in dogs, mice, and rats following oral administration and the structure determination of its metabolites by liquid chromatography/mass spectrometry and NMR spectroscopy. *Drug Metab Dispos* 34:213-224.

Billman GE (2008) The cardiac sarcolemmal ATP-sensitive potassium channel as a novel target for anti-arrhythmic therapy. *Pharmacol Ther* 120:54-70.

Clarke NJ, Rindgen D, Korfmacher WA and Cox KA (2001) Systematic LC/MS metabolite identification in drug discovery. *Anal Chem* 73:430A-439A.

Clarkson C, Staerk D, Hansen SH and Jaroszewski JW (2005) Hyphenation of solid-phase extraction with liquid chromatography and nuclear magnetic resonance: application of HPLC-DAD-SPE-NMR to identification of constituents of Kanahia laniflora. *Anal Chem* 77:3547-3553.

Corcoran O and Spraul M (2003) LC-NMR-MS in drug discovery. *Drug Discov Today* 8:624-631.

de Tullio P, Becker B, Boverie S, Dabrowski M, Wahl P, Antoine MH, Somers F, Sebille S, Ouedraogo R, Hansen JB, Lebrun P and Pirotte B (2003) Toward tissue-selective pancreatic B-cells KATP channel openers belonging to 3-alkylamino-7-halo-4H-1,2,4-benzothiadiazine 1,1-dioxides. *J Med Chem* 46:3342-3353.

de Tullio P, Boverie S, Becker B, Antoine MH, Nguyen QA, Francotte P, Counerotte S, Sebille S, Pirotte B and Lebrun P (2005) 3-Alkylamino-4H-1,2,4-benzothiadiazine 1,1-dioxides as ATP-sensitive potassium channel openers: effect of 6,7-disubstitution on potency and tissue selectivity. *J Med Chem* 48:4990-5000.

Hambrock A, Loffler-Walz C, Kloor D, Delabar U, Horio Y, Kurachi Y and Quast U (1999) ATP-Sensitive K+ channel modulator binding to sulfonylurea receptors SUR2A and SUR2B: opposite effects of MgADP. *Mol Pharmacol* 55:832-840.

Hansen JB (2006) Towards selective Kir6.2/SUR1 potassium channel openers, medicinal chemistry and therapeutic perspectives. *Curr Med Chem* 13:361-376.

Inagaki N, Gonoi T, Clement JPt, Namba N, Inazawa J, Gonzalez G, Aguilar-Bryan L, Seino S and Bryan J (1995) Reconstitution of IKATP: an inward rectifier subunit plus the sulfonylurea receptor. *Science* 270:1166-1170.

Ko EA, Han J, Jung ID and Park WS (2008) Physiological roles of K+ channels in vascular smooth muscle cells. *J Smooth Muscle Res* 44:65-81.

Lawson K (1996) Potassium channel activation: a potential therapeutic approach? *Pharmacol Ther* 70:39-63.

Lebrun P, Antoine MH, Ouedraogo R, Herchuelz A, de Tullio P, Delarge J and Pirotte B (1997) Pyridothiadiazines as potent inhibitors of glucose-induced insulin release. *Adv Exp Med Biol* 426:145-148.

Miki T, Nagashima K and Seino S (1999) The structure and function of the ATP-sensitive K+ channel in insulin-secreting pancreatic beta-cells. *J Mol Endocrinol* 22:113-123.

Oliveira EJW, D.G. (2000) Liquid chromatography-mass spectrometry in the study of the metabolism of drugs and other xenobiotics. *Biomed. Chromatogr.* 14:351-372.

Pirotte B, Antoine MH, de Tullio P, Hermann M, Herchuelz A, Delarge J and Lebrun P (1994) A pyridothiadiazine (BPDZ 44) as a new and potent activator of ATP-sensitive K+ channels. *Biochem Pharmacol* 47:1381-1386.

Raffa L LL, Grana E. (1965) Azione cardiovasolare di derivati del 1,2,4-benzotiadiazin-1,1-diossido, nota II. *Il Farmaco* 20:647-661.

Rasmussen SB, Sorensen TS, Hansen JB, Mandrup-Poulsen T, Hornum L and Markholst H (2000) Functional rest through intensive treatment with insulin and potassium channel openers preserves residual beta-cell function and mass in acutely diabetic BB rats. *Horm Metab Res* 32:294-300.

Sandvoss M, Bardsley B, Beck TL, Lee-Smith E, North SE, Moore PJ, Edwards AJ and Smith RJ (2005) HPLC-SPE-NMR in pharmaceutical development: capabilities and applications. *Magn Reson Chem* 43:762-770.

Silva Elipe MV (2003) Advantages and disadvantages of nuclear magnetic resonance spectroscopy as a hyphenated technique. *Analytica Chimica Acta* 497:1-25.

Simpson AJ, Tseng LH, Simpson MJ, Spraul M, Braumann U, Kingery WL, Kelleher BP and Hayes MH (2004) The application of LC-NMR and LC-SPE-NMR to compositional studies of natural organic matter. *Analyst* 129:1216-1222.

Tatsis EC, Boeren S, Exarchou V, Troganis AN, Vervoort J and Gerothanassis IP (2007) Identification of the major constituents of Hypericum perforatum by LC/SPE/NMR and/or LC/MS. *Phytochemistry* 68:383-393.

Waxman DJ and Azaroff L (1992) Phenobarbital induction of cytochrome P-450 gene expression. *Biochem J* 281 (Pt 3):577-592.

Wilson SR, Malerod H, Petersen D, Simic N, Bobu MM, Rise F, Lundanes E and Greibrokk T (2006) Short communication controlling LC-SPE-NMR systems. *J Sep Sci* 29:582-589.

Yang Z (2006) Online hyphenated liquid chromatography-nuclear magnetic resonance spectroscopy-mass spectrometry for drug metabolite and nature product analysis. *J Pharm Biomed Anal* 40:516-527.

Footnotes

This study was supported by grants from the National Fund for Scientific Research (F.N.R.S., Belgium) from which P. de Tullio and M. Frédérich are Senior Research Associates and P. Lebrun is Research Director.

DMD Fast Forward. Published on October 29, 2009 as DOI: 10.1124/dmd.109.028928
This article has not been copyedited and formatted. The final version may differ from this version.

Legends for figures

Figure 1: K_{ATP} channel openers belonging to 3-alkylamino-4*H*-1,2,4-pyrido- and 3-alkylamino-4*H*-1,2,4-benzothiadiazine 1,1-dioxides.

Figure 2: Metabolic profile of compound BPDZ 157

Column: Alltech Hypersil BDS C18 (150 x 4.6 mm, i.d.; particle size = 3 µm). Other conditions: see Experimental section

Legend: · · · · · · BPDZ 157 not metabolized; —————— BPDZ 157 metabolized; ------ Gradient in acetonitrile.

Figure 3: (A) Product ion spectrum of the protonated molecule ($[M+H]^+$ at *m/z* = 302) obtained from the chromatographic peak corresponding to BPDZ 157 - Collision energy = 20 eV. Other conditions: see Experimental section. (B): BPDZ 157 fragmentation pathway. (C) Putative structures of the BPDZ 157 metabolites according to the LC-MS/MS analysis.

Figure 4: ^{1}H NMR (classical 30° pulse) spectra of BPDZ 157 and its metabolites M1 to M5.

Figure 5: (A) potential stereoisomers of M4 and M5. (B) structures of the BPDZ 157 metabolites resulting from LC-MS/MS and NMR analysis.

Figure 6: Metabolic profile of compound BPDZ 73

Column: Alltech Hypersil BDS C18 (150 x 4.6 mm, i.d.; particle size = 3 µm). Other conditions: see Experimental section

Legend: · · · · · · · · ·BPDZ 73 not metabolized; ——— BPDZ 73 metabolized; ------ Gradient in acetonitrile.

DMD Fast Forward. Published on October 29, 2009 as DOI: 10.1124/dmd.109.028928
This article has not been copyedited and formatted. The final version may differ from this version.

Table 1: MS/MS data of BPDZ 157 and its metabolites.

	Protonated molecule	**Product ions**
BPDZ 157 (parent)	302.0730 $[C_{12}H_{16}ClN_3O_2S]^+$	231.9956 $[C_7H_7ClN_3O_2S]^+$ 189.9645 $[C_6H_5ClNO_2S]^+$ 141.9986 $[C_7H_9ClN]^+$ 126.0045 $[C_6H_6ClN]^+$
M1	231.9947 $[C_7H_7ClN_3O_2S]^+$	189.9675 $[C_6H_5ClNO_2S]^+$ 142.0032 $[C_7H_9ClN]^+$ 126.0092 $[C_6H_6ClN]^+$
M2	334.0628 $[C_{12}H_{16}ClN_3O_4S]^+$	316.0504 $[C_{12}H_{14}ClN_3O_3S]^+$ 298.0374 $[C_{12}H_{12}ClN_3O_2S]^+$ 272.0240 $[C_{10}H_{12}ClN_3O_2S]^+$ 231.9908 $[C_7H_7ClN_3O_2S]^+$ 189.9695 $[C_6H_5ClNO_2S]^+$ 142.0008 $[C_7H_9ClN]^+$ 126.0086 $[C_6H_6ClN]^+$
M3	318.0679 $[C_{12}H_{16}ClN_3O_3S]^+$	300.0471 $[C_{12}H_{14}ClN_3O_2S]^+$ 231.9775 $[C_7H_7ClN_3O_2S]^+$ 189.9552 $[C_6H_5ClNO_2S]^+$ 141.9969 $[C_7H_9ClN]^+$ 125.9960 $[C_6H_6ClN]^+$
M4	318.0679 $[C_{12}H_{16}ClN_3O_3S]^+$	300.0495 $[C_{12}H_{14}ClN_3O_2S]^+$ 231.9747 $[C_7H_7ClN_3O_2S]^+$ 189.9529 $[C_6H_5ClNO_2S]^+$ 141.9940 $[C_7H_9ClN]^+$ 125.9997 $[C_6H_6ClN]^+$
M5	318.0679 $[C_{12}H_{16}ClN_3O_3S]^+$	300.0495 $[C_{12}H_{14}ClN_3O_2S]^+$ 231.9747 $[C_7H_7ClN_3O_2S]^+$ 189.9529 $[C_6H_5ClNO_2S]^+$ 141.9940 $[C_7H_9ClN]^+$ 125.9997 $[C_6H_6ClN]^+$
M6	316.0522 $[C_{12}H_{14}ClN_3O_3S]^+$	299,0306 $[C_{12}H_{13}ClN_3O_2S]^+$ 231.9795 $[C_7H_7ClN_3O_2S]^+$ 189.9682 $[C_6H_5ClNO_2S]^+$ 142.0004 $[C_7H_9ClN]^+$ 126.0083 $[C_6H_6ClN]^+$

DMD Fast Forward. Published on October 29, 2009 as DOI: 10.1124/dmd.109.028928
This article has not been copyedited and formatted. The final version may differ from this version.

Table 2: ^{1}H NMR chemical shift assignments of BPDZ 157 and its metabolites in ACN-*d3*

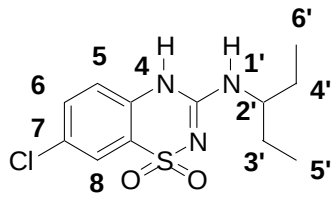

BPDZ 157 (4)

Position	δ_H (multiplicity, integration, Cosy H-H correlation or *J* in Hz)					
	BPDZ 157	**M1**	**M2**	**M3**	**M4**	**M5**
4	8.87 (bs, 1H)	8.98 (bs, 1H)	8.97 (bs, 1H)	8.77 (bs, 1H)	8.82 (bs, 1H)	8.70 (bs, 1H)
5	7.14 (d, 1H, 8.35 Hz)	7.01 (d, 1H, 6)	7.09 (d, 1H, 6)	7.04 (d, 1H, 6)	7.10 (d, 1H, 6)	6.96 (d, 1H)
6	7.53 (d, 1H, 8.67 Hz)	7.42 (d, 1H, 5)	7.54 (d, 1H, 5)	7.45 (d, 1H, 5)	7.51 (d, 1H, 5)	7.40 (d, 1H)
8	7.75 (s, 1H)	7.65 (s, 1H)	7.76 (s, 1H)	7.67 (s, 1H)	7.73 (s, 1H)	7.60 (s, 1H)
1'	5.65 (bs, 1H)	5.75 (s, 2H)	6.07 (bs, 1H)	5.83 (bs, 1H)	5.75 (bs, 1H, 2')	5.65 (bs, 1H)
2'	3.79 (bm, 1H)	-	3.66 (bs, 1H, 1')	3.85 (bs, 1H)	3.75 (bs, 1H, 1')	3.59 (bs, 1H)
3'	1.64 (m, 2H, 7.35 Hz)	-	3.96 (bm, 1H, 5')	1.74 (m, 2H, 5')	3.85 (bs, 1H, 5')	3.75 (bs, 1H)
4'	1.52 (m, 2H, 7.55 Hz)	-	4.32 (bm, 1H, 6')	1.51 (m, 2H, 6')	1.67 (bs, 1H, 6') 1.44 (m, 1H, 6')	1.48 (m, 2H)
5'	0.95 (t, 3H, 7.4 Hz)	-	1.25 (d, 3H, 3')	3.56 (bs, 2H, 3')	1.13 (d, 3H, 3')	1.03 (d, 3H)
6'	0.95 (t, 3H, 7.4 Hz)	-	1.15 (d, 3H, 4')	0.85 (t, 3H, 4')	0.95 (t, 3H, 4')	0.84 (t, 3H)
OH	-	-	3.39 (bs, 2H)	2.90 (bs, 1H)	3.80 (bs, 1H)	3.41 (bs, 1H)

Figure 1.

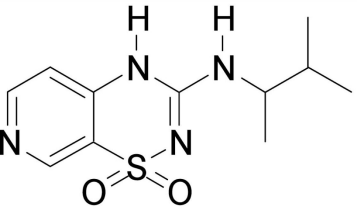

BPDZ 44 (1)

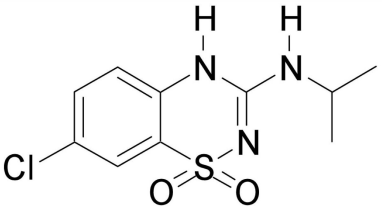

BPDZ 73 (2)

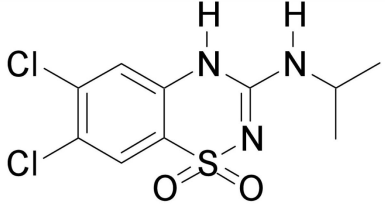

BPDZ 154 (3)

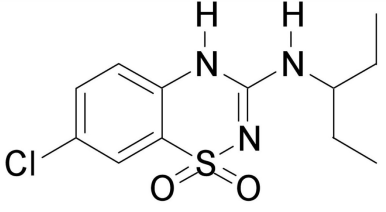

BPDZ 157 (4)

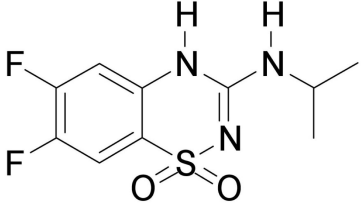

BPDZ 415 (5)

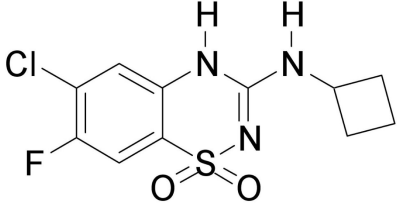

BPDZ 256 (6)

Figure 2.

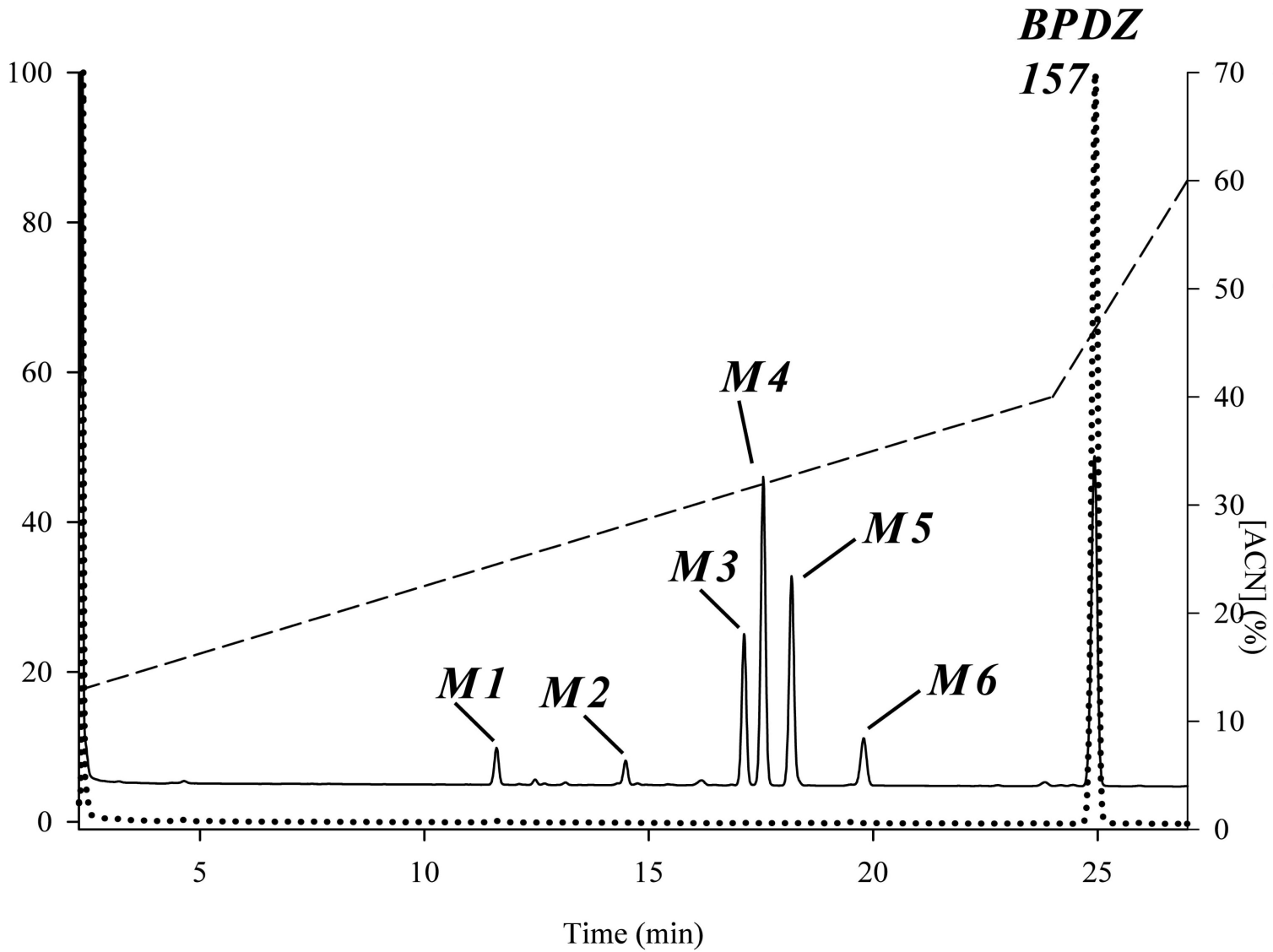

Figure 3.

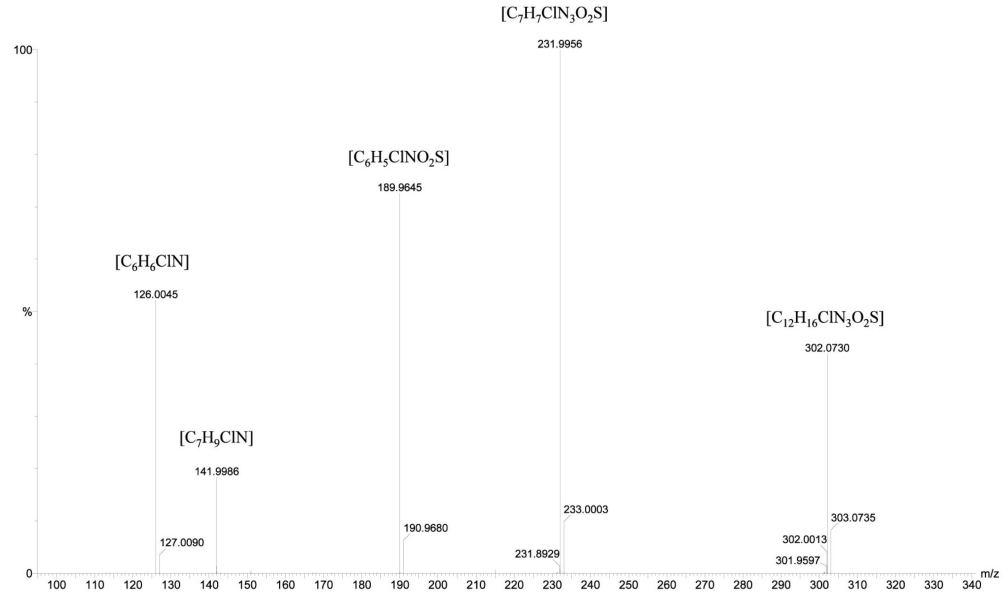

A

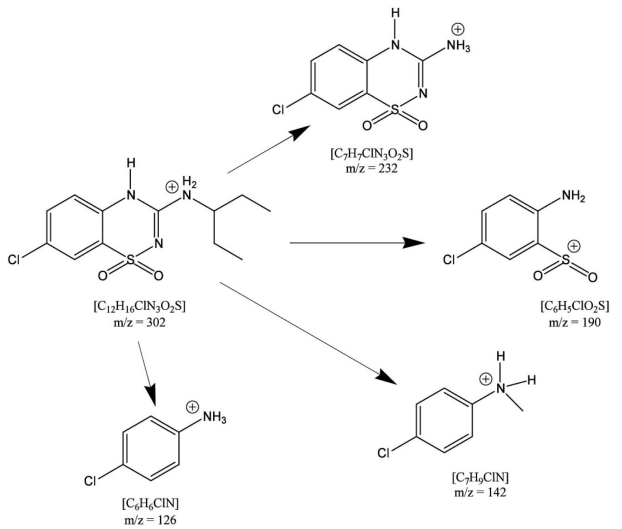

B

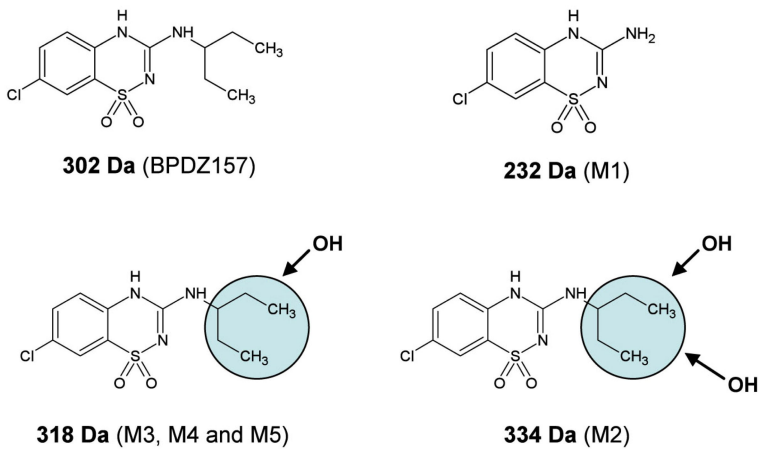

C

Figure 4.

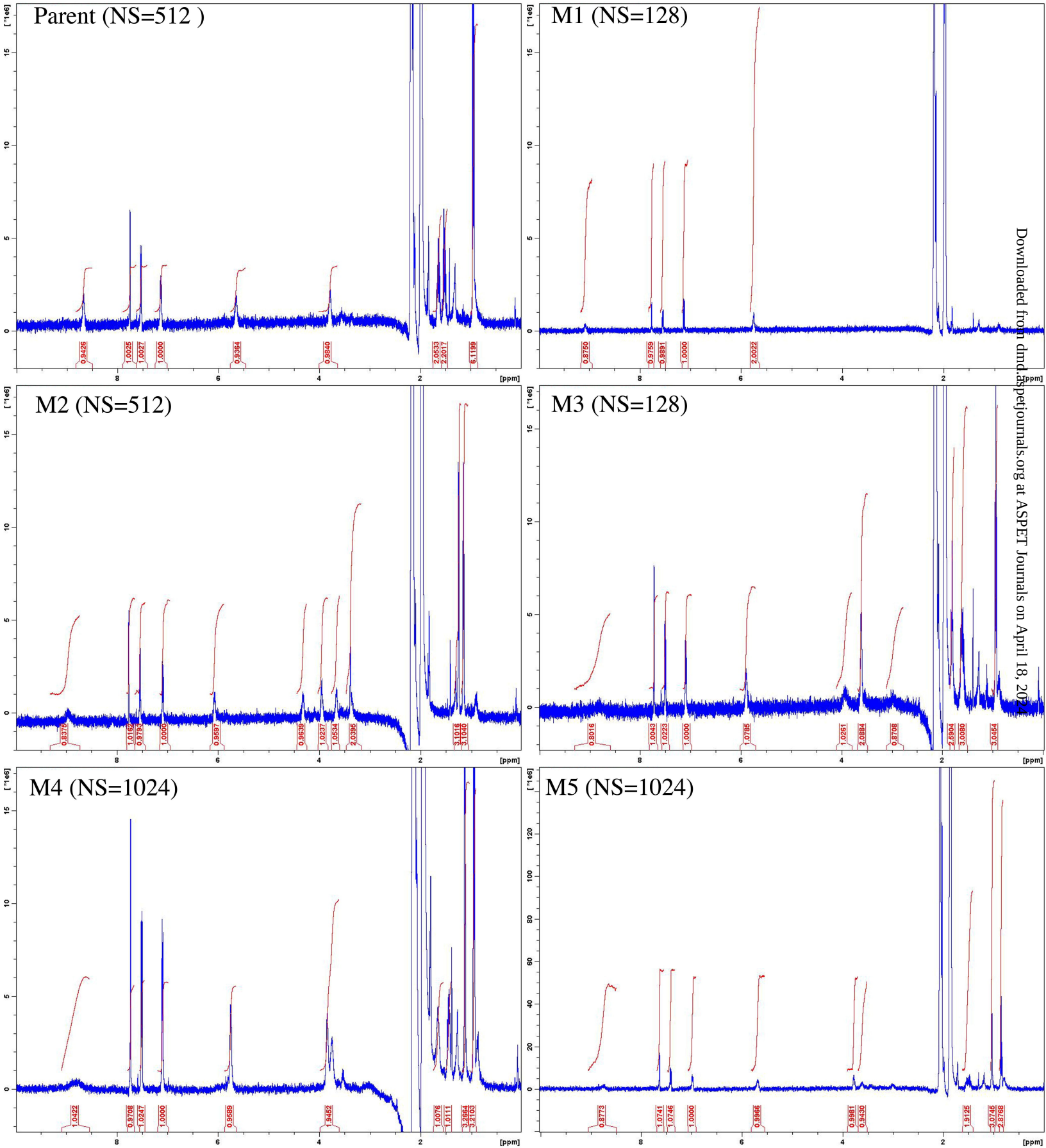

DMD Fast Forward. Published on October 29, 2009 as DOI: 10.1124/dmd.109.028928
This article has not been copyedited and formatted. The final version may differ from this version.

Figure 5.

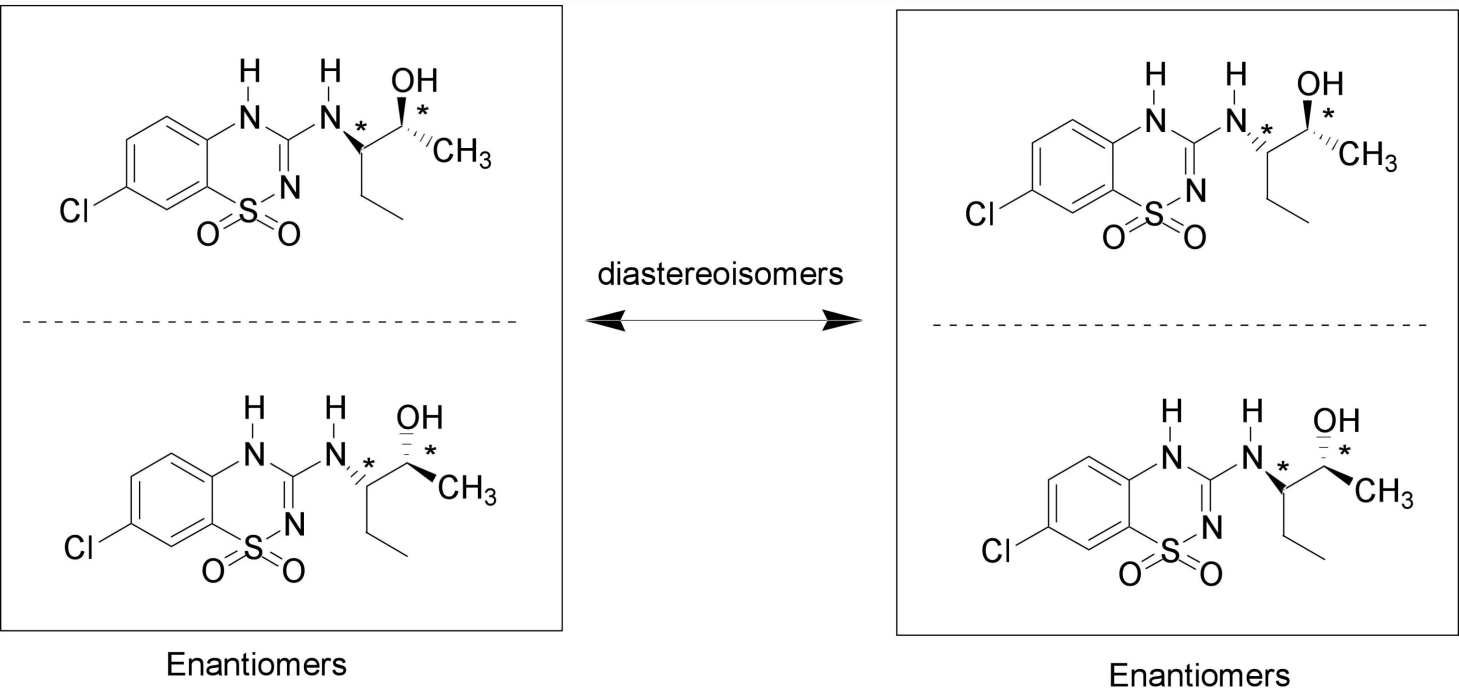

A

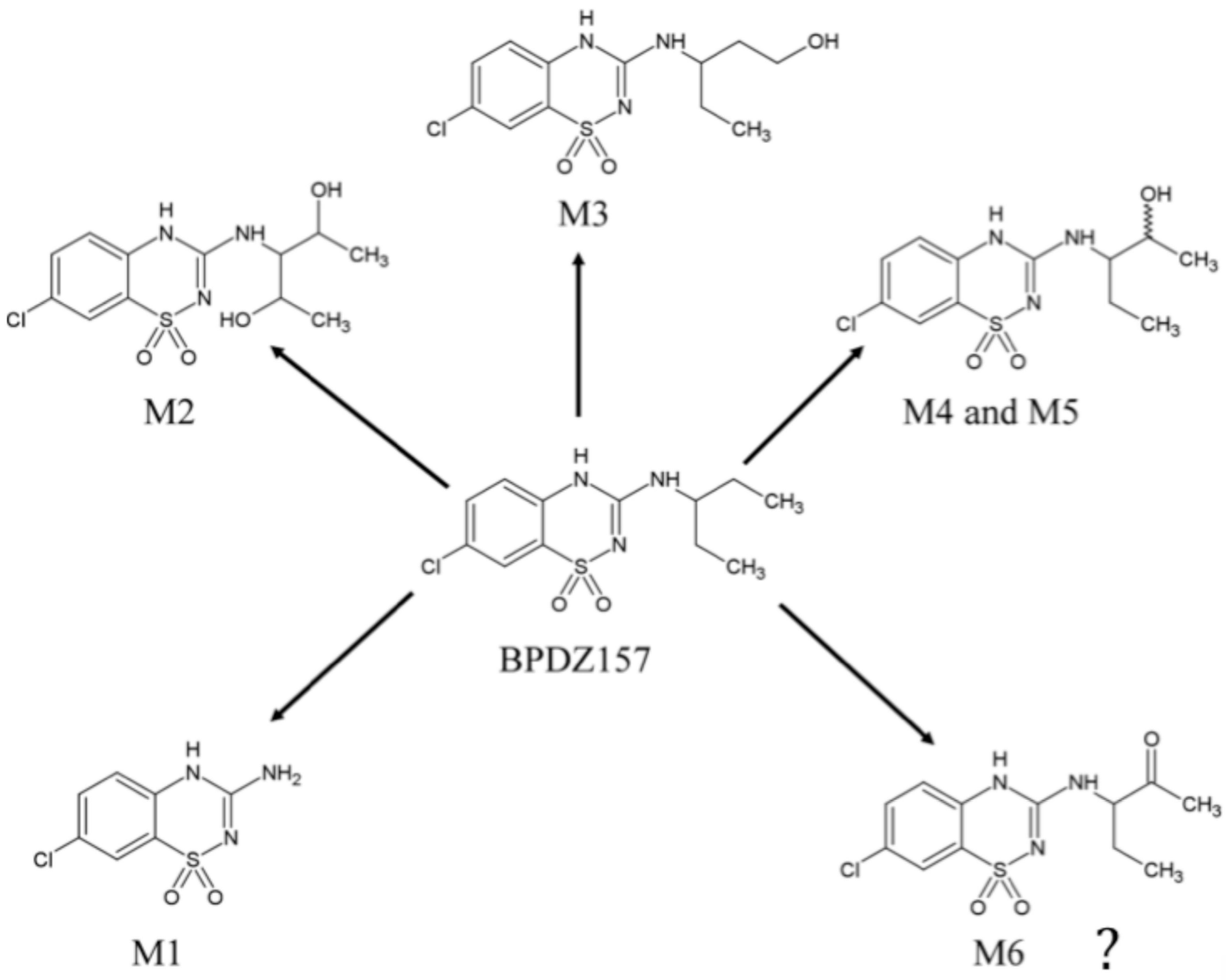

B

Figure 6.

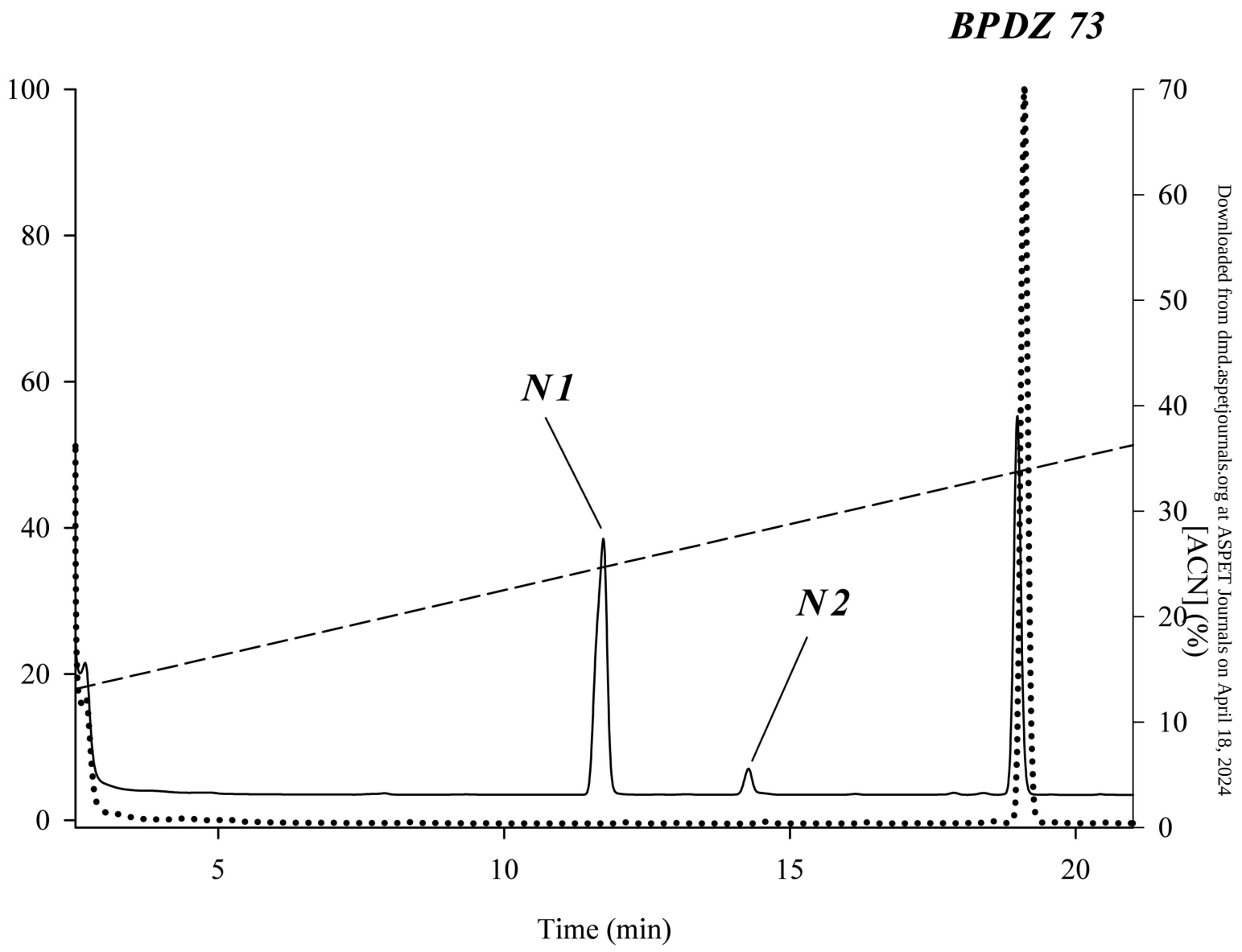

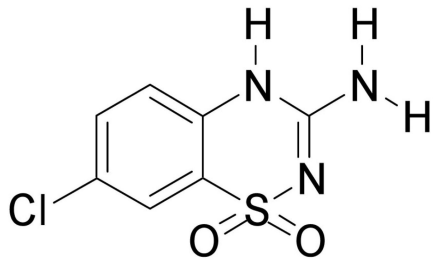

N1

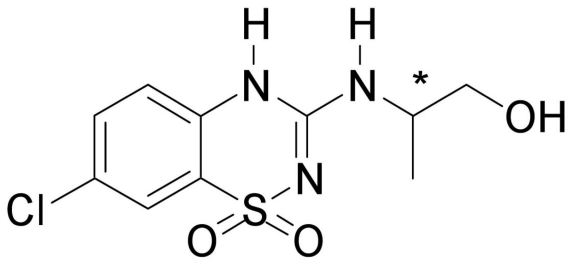

N2